Fragmentation Reactions of a_2 Ions Derived From Deprotonated Dipeptides—A Synergy Between Experiment and Theory†

Gregory A. Chass, Christopher N. J. Marai, Alex G. Harrison,* and Imre G. Csizmadia

Department of Chemistry, University of Toronto, Toronto, Ontario M5S 3H6, Canada

Received: April 3, 2002; In Final Form: June 13, 2002

The fragmentation reactions of a number of a_2 ions ($[M-H-CO_2]^-$) derived from dipeptides have been studied by energy-resolved mass spectrometry, isotopic labeling, and MS^3 experiments. The general reaction sequence

$$H_2N-CH(R_1)-C(=O)-N(R_2)-CHR_3^- \rightarrow {}^-HN-CH(R_1)-C(=O)-N(R_2)-CH_2R_3 \quad (1)$$

$$^-HN-CH(R_1)-C(=O)-N(R_2)-CH_2R_3 \rightarrow R_3CH_2-N(R_2)-C=O^- + HN=CHR_1 \quad (2)$$

$$R_3CH_2-N(R_2)-C=O^- \rightarrow R_3CH_2-N(R_2)^- + CO \quad (3)$$

leading eventually to a deprotonated amine, is shown to occur, a reaction sequence first proposed by Styles and O'Hair (*Rapid Commun. Mass Spectrom.* **1998**, *12*, 809) from a study of the a_2 ion derived from glycylglycine. When an amidic hydrogen (R_2 = H) is present, the initial proton-transfer reaction 1 is nonreversible. However, when there is no amidic hydrogen, as in the a_2 ions derived from H−Ala−Pro−OH or H−Gly−Sar−OH, the initial proton-transfer reaction 1 becomes reversible, leading to the interchange of N-bonded and C-bonded hydrogens. Ab initio calculations at the MP2/6-31+G(d) level of the energies and interconversion pathways of anions derived by deprotonation of glycine *N*-methylamide show a barrier of 8 kcal mol^{-1} for reaction 1, with reaction 2 being 23.8 kcal mol^{-1} endothermic. When an amidic hydrogen (R_2 = H) is present, the amine-deprotonated species formed in reaction 1 abstracts a proton from the amide nitrogen to form the amide-deprotonated species, the most stable species on the potential energy surface. The system effectively becomes trapped in this low-energy well and exits upon activation by reactions 2 and 3 as observed when glycine *N*-methylamide is deprotonated directly. When no amidic hydrogen is present, this low-energy state does not exist, and reaction 1 becomes reversible, leading to the interchange of N-bonded and C-bonded hydrogens. In these cases, a significant population of the original a_2 ion is formed, which fragments by the reaction

$$H_2N-CH(R_1)-C(=O)-N(R_2)-CHR_3^- \rightarrow H_2N-CH(R_1)-C=O^- + R_3CH=NR_2 \quad (4)$$

Introduction

Tandem mass spectrometry of protonated peptides has proven to be a useful method for determining the amino acid identities and sequences for peptides.[1−4] As a result of many studies, the main features of the fragmentation of protonated peptides have been elucidated in a general way.[5,6] A number of recent studies have been directed toward a more detailed understanding of fragmentation mechanisms and fragment ion structures; these studies have been summarized in four recent review articles.[7−10] On the other hand, much less is known concerning the fragmentation of deprotonated peptides, and much of the information that is available derives from high-energy collision-induced-dissociation (CID) studies of small deprotonated peptides,[11−22] although Beauchamp and co-workers[23] have explored the threshold dissociation reactions of a number of deprotonated peptides by Fourier transform/ion cyclotron resonance methods. With the exception of large acidic peptides, where multiple deprotonation occurs,[24−27] no species larger than deprotonated tripeptides have been studied.

A recent paper from this laboratory[28] reported a detailed study of the low-energy CID of the $[M-H]^-$ ions of a number of di- to pentapeptides containing H or alkyl α-groups. Significantly greater sequence-specific fragmentation was observed in the low-energy CID studies than was observed in previous high-energy CID studies.[16] Modifying the nomenclature used for protonated peptides,[5,6] the fragmentation reactions observed are summarized in Scheme 1. An additional reaction observed for a_n ions ($[M-H-CO_2]^-$) involved elimination of the N-terminal amino acid residue. Thus, a_3 ions derived from tripeptides eliminated the N-terminal residue, whereas a_4 ions showed sequential elimination of two amino acid residues from the N-terminus. Exchange of the labile hydrogens for deuterium showed that either a labile (N-bonded) or a nonlabile (C-bonded) hydrogen was transferred in this elimination reaction. In 1998, Styles and O'Hair[29] reported that the $[M-H-CO_2]^-$ (a_2) ion derived from diglycine also eliminated the N-terminal amino acid residue. Reasoning from the results of ^{15}N-labeling, MS/MS experiments, and ab initio calculations, they proposed the reaction sequence illustrated in general terms in Scheme 2. The present work reports a more detailed and extensive study of the fragmentation of a_2 ions using energy-resolved mass spectrometry,[30−32] MS^3 experiments, isotopic labeling, and ab

† Part of the special issue "Jack Beauchamp Festschrift".

* Address for correspondence: A. G. Harrison, Department of Chemistry, University of Toronto, 80 St. George Street, Toronto, Ontario M5S 3H6, Canada. E-mail: aharriso@chem.utoronto.ca. Tel. and Fax: (416) 978-3577.

10.1021/jp0208891 CCC: $22.00
Published on Web 08/10/2002

SCHEME 1

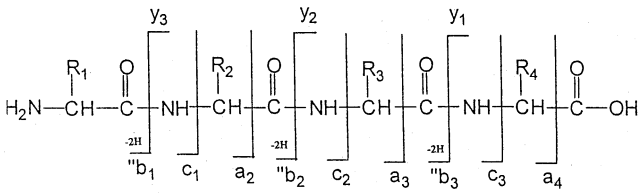

SCHEME 2

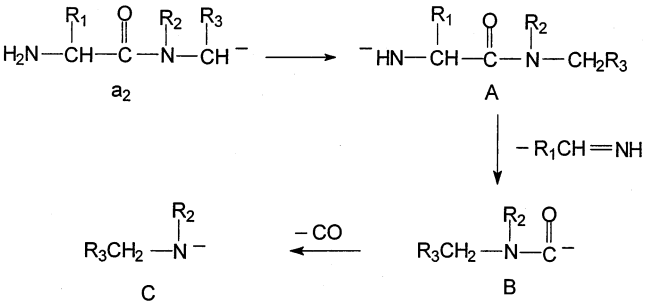

initio calculations. The present work extends the results of Styles and O'Hair both in terms of experimental observations and in terms of theoretical interpretation. In particular, the present study shows that, in contrast to the results for larger a_n ions, where either a N-bonded hydrogen or a C-bonded hydrogen can be transferred in elimination of the N-terminal amino acid residue, for a_2 ions, specifically a N-bonded hydrogen is transferred in elimination of the N-terminal residue. The reasons for this specificity for a_2 ions are explored by ab initio calculations.

Experimental Section

Collision-induced-dissociation (CID) studies were carried out using an electrospray ionization/quadrupole mass spectrometer (VG Platform, Micromass, Manchester, UK). It is well-known[33−35] that CID can be achieved in the interface region between the atmospheric-pressure ion source and the quadrupole mass analyzer, so-called cone-voltage CID. Further, it is known[36−38] that the average energy imparted to the decomposing ions increases as the field in the interface region is increased, and a number of studies[39−42] have shown that, by varying the field in steps, energy-resolved mass spectra can be obtained that are similar to those obtained by variable low-energy CID in quadrupole collision cells. The results of such studies are presented in the following either as breakdown graphs expressing the percent of total ion abundance as a function of the cone voltage, a measure of the field in the interface region, or as CID mass spectra at a specified cone voltage.

Ionization was achieved by electrospray with the sample, at micromolar concentration in 1:1 CH_3CN/1% aqueous NH_3, being introduced into the source at a flow rate of 30 μL min^{-1}. The electrospray needle was held at −2.5 to −3.0 kV. N_2 was used as both the nebulizing gas and the drying gas. The use of 1:1 CD_3CN/1% ND_3 in D_2O resulted in exchange of all labile hydrogens by deuterium and formation of the $[M-D]^-$ ion in the ionization process; with N_2 as the drying gas, no evidence for back-exchange in the interface region was observed, although such back-exchange did occur when air was used as the nebulizing and drying gas.

MS/MS/MS experiments were performed using an electrospray-triple quadrupole instrument (Sciex API III, MDS Sciex, Toronto). Fragment ions formed by CID in the interface region were mass-selected by the first quadrupole stage and underwent collisional activation in the radio-frequency-only quadrupole collision cell, with analysis of the ionic fragmentation products by the final mass-analyzing quadrupole.

All peptide samples were obtained from BACHEM Biosciences (King of Prussia, PA). CD_3CN (99.8 atom % D) and D_2O (99.9 atom % D) were obtained from Cambridge Isotope Laboratories (Andover, MA), whereas the ND_3OD (26% in D_2O, >99 atom % D) was obtained from CDN Isotopes (Pointe Claire, Quebec, Canada).

Computational Methods

Input files were constructed using a standardized and modular approach allowing for quick additions, removals, or rearrangements of any constituent nuclei without the need for the entire structure to be redefined. Therefore, any system can be modified at any time to model a new system using the preoptimized results both accurately and efficiently.

The initial peptide structures were first preoptimized with the AM1 semiempirical method[43] to quickly produce a working model. Conformers were then formed through the numeric manipulation of structural variables. Conformers were optimized with the restricted Hartree−Fock ab initio method using the 3-21G and 6-31G(d) split-valence basis sets. In the final stages, electron correlation was induced with the second-order Moller−Plesset perturbation method,[44] again using a split-valence basis set, specifically the 6-31+G(d) level of theory. Convergence criteria of 3.0×10^{-4}, 4.5×10^{-4}, 1.2×10^{-3}, and 1.8×10^{-3} were used for the gradients of the RMS (root-mean-square) force, maximum force, RMS displacement, and maximum displacement vectors, respectively.

Multidimensional conformation analysis (MDCA)[45] was used to characterize the topologically probable set of structures for each structure computed. Geometry optimizations were performed on each conformer and run through all three levels of theory in the above order. The input for each conformer made use of the output geometry of the preceding level to formulate the geometry for the next higher level. If a conformer failed to satisfy a convergence threshold for any level of theory, the implicated dihedral angle that fell outside the expected range was reset to its ideal value for reoptimization.

Transition state structures were located and optimized through use of the QST2 method,[46] starting from the preoptimized structures of the minima on either side of the first-order saddle point. All structural minima and first-order saddle points were characterized by vibrational frequency calculations to ensure that each minimum had all real frequencies and that transition state structures had one imaginary frequency.

Zero-point energies were computed and adjusted by an appropriate correction factor of 0.967 for the MP2/6-31+G(d) level of theory.[47] The zero-point-corrected energies were then combined with the total energies resulting from the geometry optimizations. This method effectively raises the energy of each structure, resulting in a more accurate energetic description for each conformer and transition state computed. Qualitatively, the results are not perturbed to a significant extent; however, theory demands quantitatively precise evaluations of these energetic profiles.

Vibrational scale factors do not differ very much at a given level of theory when similar basis sets are compared. For example, the conversion factor is 0.8953 at HF/6-31G(d) and 0.8970 at HF/6-31+G(d) level of theory. Similarly, at the MP2 level of theory, including both full- and frozen-core approaches, the values range from 0.9370 to 0.9434 using three variants of the 6-31G basis set.[47] This difference, 0.9434 − 0.9370, represents a 0.64 cm^{-1} difference for a 100 cm^{-1} vibrational

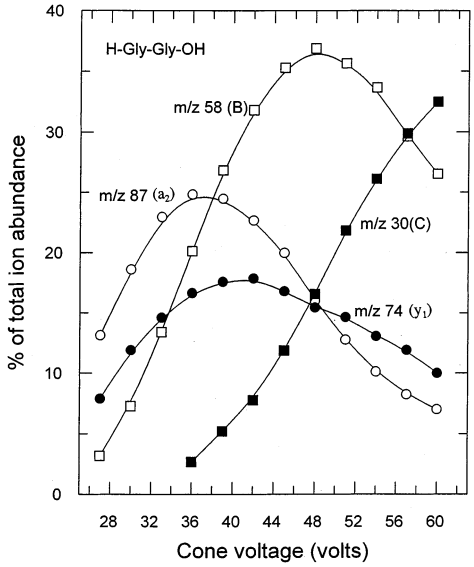

Figure 1. Breakdown graph for deprotonated Gly-Gly.

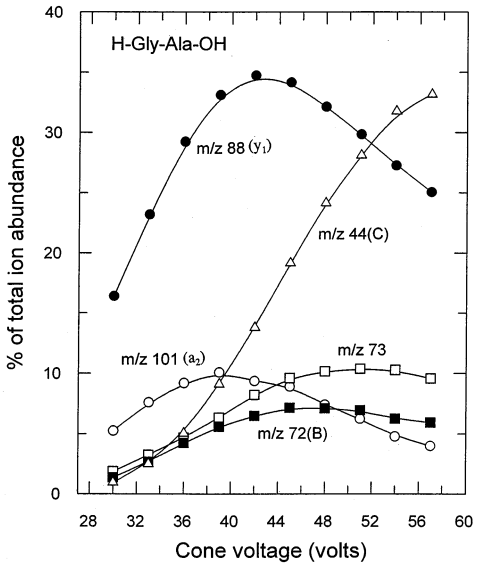

Figure 2. Breakdown graph for deprotonated Gly-Ala.

frequency and 0.0064 kcal mol^{-1} for every 1-kcal zero-point-energy (ZPE) correction. For this reason, it seemed prudent to use the correction value (0.967) used by Styles and O'Hair[29] so that the comparison could be made more directly

Results and Discussion

Figure 1 shows the breakdown graph obtained by cone-voltage CID for the $[M-H]^-$ ion of glycylglycine. The ionic fragments are labeled in consistency with Schemes 1 and 2. Primary fragmentation of the $[M-H]^-$ ion occurs to form the y_1 ion and the a_2 ion (CO_2 loss) as elucidated in earlier studies.[16,28,29] The breakdown graph clearly shows sequential fragmentation of the a_2 ion to produce *m/z* 58 ($[CH_3NHCO]^-$) and *m/z* 30 ($[CH_3NH]^-$). The results are thus consistent with the mechanism proposed by Styles and O'Hair[29] and outlined in general terms in Scheme 2.

A more detailed study was carried out for the $[M-H]^-$ (*m/z* 145) ions derived from H−Gly−Ala−OH and H−Ala−Gly−OH. Figures 2 and 3 show the breakdown graphs obtained by cone-voltage CID with the fragment ions again identified in terms of Schemes 1 and 2. The CID mass spectra of the mass-

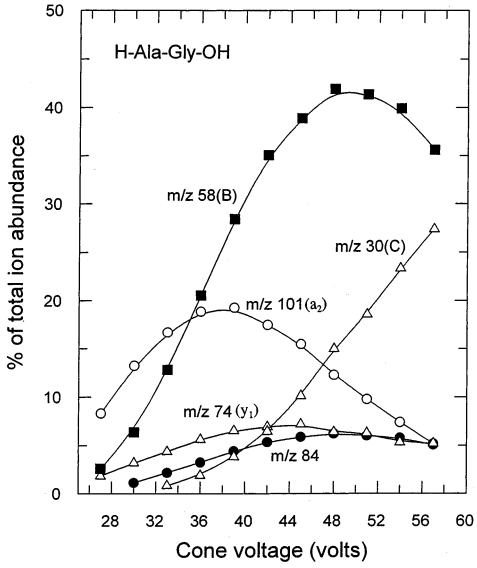

Figure 3. Breakdown graph for deprotonated Ala-Gly.

TABLE 1: CID of $[M-H]^-$ Ions at 3-eV Center-of-Mass Collision Energy

ion	Gly-Ala intensity (*m/z*)	Ala-Gly intensity (*m/z*)
a_2	36.6(101)	100(101)
y_1	100(88)	31.1(74)
a_2-NH_3		22.8(84)
c_1	19.1(73)	
B	9.0(72)	61.9(58)
C	7.6(44)	9.7(30)

selected $[M-H]^-$ ions obtained at 3 eV center-of-mass collision energy on the triple-quadrupole instrument are presented in Table 1 and show the same fragment ions as observed in the cone-voltage CID studies. Not unexpectedly, the y_1 ion is more prominent in the fragmentation of deprotonated H−Gly−Ala−OH than it is in the fragmentation of deprotonated H−Ala−Gly−OH because a more stable deprotonated amino acid is formed. The a_2 ions (*m/z* 101) fragment as indicated in general terms by Scheme 2. Thus, the a_2 ion derived from H−Ala−Gly−OH shows fragmentation to $[CH_3NHCO]^-$ (*m/z* 58) and $[CH_3NH]^-$ (*m/z* 30), whereas the a_2 ion derived from H−Gly−Ala−OH fragments to form $[CH_3CH_2NHCO]^-$ (*m/z* 72) and $[CH_3CH_2NH]^-$ (*m/z* 44), although the initial B ion is more intense in the former case than in the latter case. These reaction pathways are confirmed by MS^3 experiments on the respective a_2 ions at 3 eV center-of-mass collision energy. The a_2 ion derived from H−Ala−Gly−OH showed minor fragmentation by loss of NH_3 to give *m/z* 84 (13.0%) with the major fragmentation route being the formation of *m/z* 58 (B) (69.6%) and *m/z* 30 (C) (17.4%), whereas the a_2 ion derived from H−Gly−Ala−OH showed formation of *m/z* 73 (presumably the c_1 ion) (14.5%) as well as *m/z* 72 (B) (20.1%) and *m/z* 44 (C) (65.4%). It is clear that the B ion formed in the latter system undergoes more facile loss of CO than does the B ion derived from H−Ala−Gly−OH.

Further support for the general mechanism of Scheme 2 comes from deuterium labeling. Figure 4 compares the CID mass spectrum of the $[M-H]^-$ ion of H−Ala−Val−OH with the CID mass spectrum of the $[M-D]^-$ ion of the dipeptide in which the labile hydrogens have been exchanged for deuterium. As expected, the a_2 ion specifically incorporates three labile hydrogens, and the y_1 ion incorporates one labile hydrogen as observed earlier.[16,28] The latter observation has been rational-

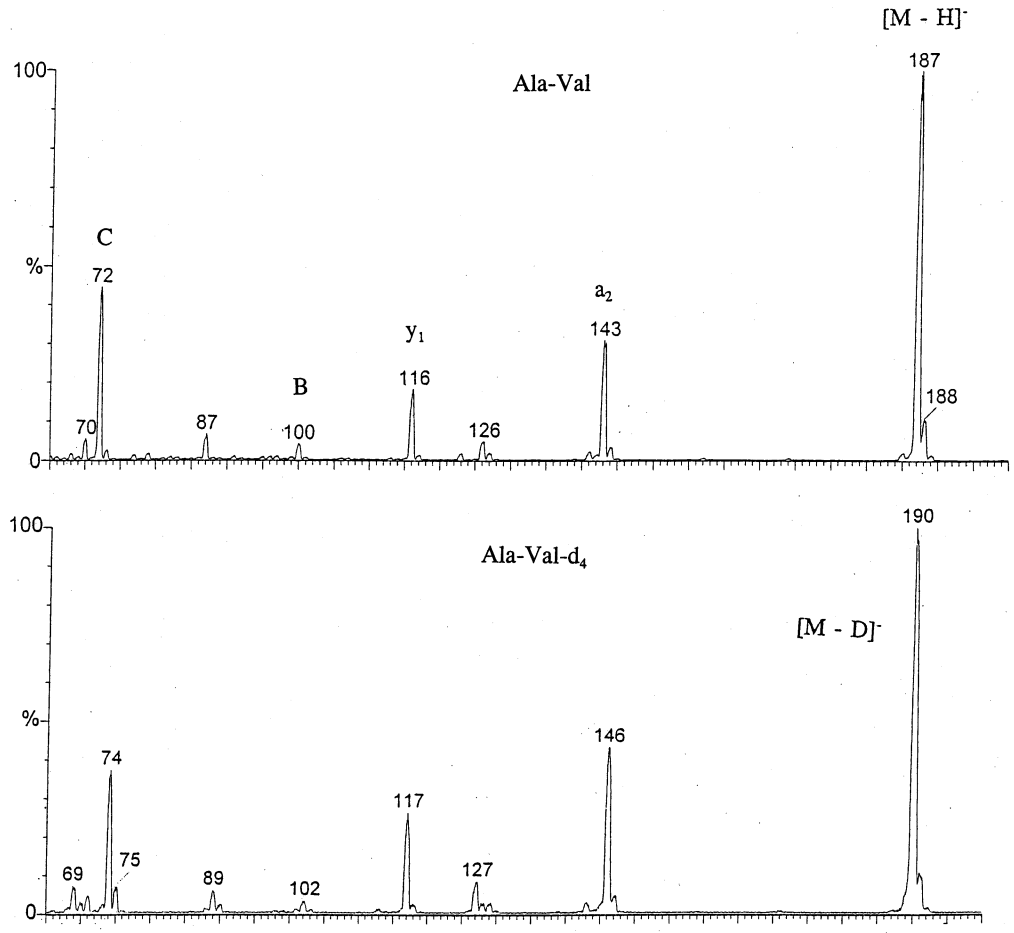

Figure 4. Comparison of CID mass spectra of $[M-H]^-$ of Ala-Val and $[M-D]^-$ of Ala-Val-d_4 (45-V cone voltage).

SCHEME 3

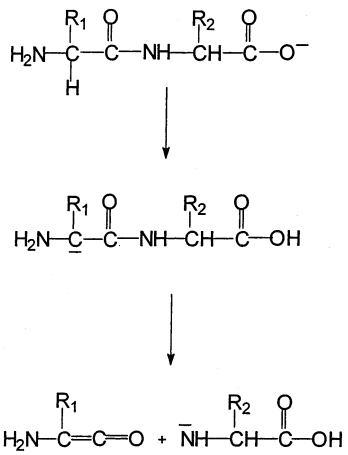

ized[16] in terms of proton transfer from the enolic position in the carboxyl-deprotonated species and elimination of a neutral ketene as outlined in Scheme 3. In support of Scheme 2, the B ion (*m*/*z* 100, [*i*-$PrCH_2NHCO]^-$) and the C ion (*m*/*z* 72, [*i*-$PrCH_2NH]^-$) both incorporate largely two labile hydrogens. Similar results (not shown) were obtained for H−Ala−Gly−OH and H−Gly−Ala−OH when the labile hydrogens were exchanged for deuterium. The specific transfer of a N-bonded hydrogen in elimination of the N-terminal amino acid residue from a_2 ions is in contrast to the results for elimination of the N-terminal amino acid residue from a_3 and a_4 ions, where either a N-bonded or a C-bonded hydrogen is transferred.[28] The spectrum in Figure 4 also shows loss of NH_3 from the a_2 ion, resulting in the species with *m*/*z* 126; this is similar to the loss of NH_3 from the a_2 ion derived from H−Ala−Gly−OH (see above). The labeling results (Figure 4) show that mainly two labile hydrogens are lost in this fragmentation process. Presumably, this fragmentation involves remote loss of NH_3 from the N-terminus incorporating one hydrogen from the alkyl side chain. The spectrum of Figure 4 also shows minor formation of the c_1 (*m*/*z* 87) ion similar to the formation of the c_1 (*m*/*z* 73) ion for the a_2 ion derived from H−Gly−Ala−OH (see above). This reaction corresponds, nominally, to elimination of a carbene from the a_2 ion. However, the labeling results (Figure 4) show incorporation of only two labile hydrogens rather than the expected three, so the reaction is clearly more complex and probably involves hydrogen migrations and rearrangements so that a more stable olefin can be eliminated.

The reaction sequence indicated by Scheme 2 proved to be general for a_2 ions derived from dipeptides containing H or alkyl α-groups, including dipeptides containing proline. As an example of the latter, Figure 5 compares the CID mass spectrum of the $[M-H]^-$ ion derived from H−Pro−Val−OH with the CID mass spectrum of the $[M-D]^-$ ion of the deuterium-labeled dipeptide. The low-intensity *m*/*z* 100 ion signal corresponds to the B ion of Scheme 2, whereas the more intense *m*/*z* 72 corresponds to the C ion ([*i*-$PrCH_2NH]^-$) and clearly incorporates both labile hydrogens present in the a_2 ion of the deuterated peptide.

A somewhat more complex result is obtained when the a_2 ion does not bear a hydrogen on the amidic nitrogen. Figure 6 compares the CID mass spectrum of the $[M-H]^-$ ion of H−Ala−Pro−OH with that of the $[M-D]^-$ ion of the dipeptide

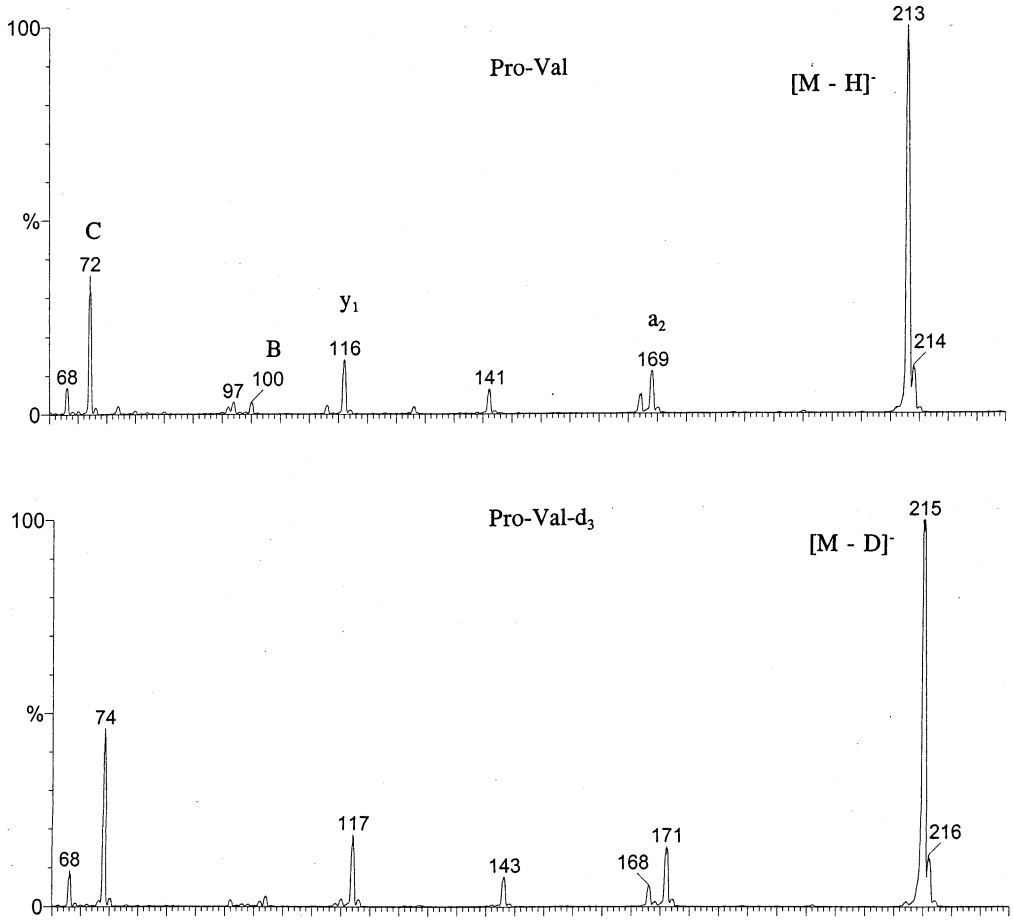

Figure 5. Comparison of CID mass spectra of $[M-H]^-$ of Pro-Val and $[M-D]^-$ of Pro-Val-d_3 (48-V cone voltage).

in which the labile hydrogens had been exchanged for deuterium. In the upper spectrum, the *m*/*z* 98 ion signal corresponds to the B ion, and the *m*/*z* 70 ion signal corresponds to the C ion of Scheme 2. The pathway of Scheme 2 should result in the incorporation of one labile hydrogen in each of these two fragments. However, as the results for the labeled dipeptide show, significant incorporation of two deuteriums occurs in both the B and C ions. Clearly, when there is no amidic hydrogen, the proton transfer from nitrogen to carbon in the first step of Scheme 2 becomes reversible. The spectrum of the unlabeled dipeptide shows a small but distinct ion signal at *m*/*z* 72. This probably arises by the pathway outlined in Scheme 4.

Figure 7 shows the breakdown graph for deprotonated H−Gly−Sar−OH, another peptide that does not contain an amidic hydrogen. The a_2 (*m*/*z* 101) ion is a major primary fragmentation product and clearly fragments further as per Scheme 2 to give *m*/*z* 72 (B) and *m*/*z* 44 (C). As Figure 8 shows, CID of the $[M-D]^-$ ion of the deuterium-labeled analogue shows significant incorporation of two labile hydrogens in the B and C product ions, similar to the results of Figure 6, indicating again that, when no amidic hydrogen is present, the first proton-transfer reaction of Scheme 2 becomes reversible. The breakdown graph also shows a significant ion signal at *m*/*z* 58, observed at *m*/*z* 58, 59, and 60 in the labeled compound; this fragment appears to arise by a pathway analogous to Scheme 4 involving elimination of $CH_3N{=}CH_2$ from the a_2 ion. Fragmentation of the $[M-H]^-$ ion also leads to a product of *m*/*z* 56, remaining largely at *m*/*z* 56 in the deuterium-labeled peptide. MS^3 experiments showed that this product originated by fragmentation of the a_2 (*m*/*z* 101) ion. A possible, but highly speculative, pathway to this product is shown in Scheme 5.

Thus, we have the situation that, when an amidic hydrogen is present in the a_2 ion, the initial proton-transfer reaction of Scheme 2 is nonreversible, whereas when no amidic hydrogen is present in the a_2 ion, as in the a_2 ions from H−Ala−Pro−OH and H−Gly−Sar−OH, the initial proton-transfer reaction becomes reversible. Ab initio calculations, discussed in detail in the following section, indicate that, when an amidic hydrogen is present, the ion A readily abstracts the amidic proton, leading to $H_2NCH(R_1)C(=O)N^-CH_2R_3$, the most stable species. Even if this proton-transfer process is reversible, it does not lead to the interchange of labile and nonlabile (C-bonded) hydrogens. This theoretical observation suggested that the $[M-H]^-$ ion of $H_2NCH_2C(=O)NHCH_3$ might fragment in a fashion similar to that of the a_2 ion derived from glycylglycine. Figure 9 shows the breakdown graph obtained for deprotonated H−Gly−$NHCH_3$ (*m*/*z* 87). Deuterium labeling showed that a labile hydrogen was removed in the ionization process, most likely the amidic hydrogen, which is the most acidic. Clearly, the *m*/*z* 87 ion fragments to form *m*/*z* 58 (B), which then loses CO to form *m*/*z* 30 (C). Also observed at higher collision energies is an ion signal at *m*/*z* 42, presumably $[NCO]^-$; the pathway to this product is uncertain.

Theoretical Considerations. Extensive ab initio calculations were carried out at the (frozen-core) MP2/6-31+G(d) level for the anions that can be derived from deprotonation of glycine *N*-methylamide and for the barriers for interconversion between these anions. The results of these calculations are summarized

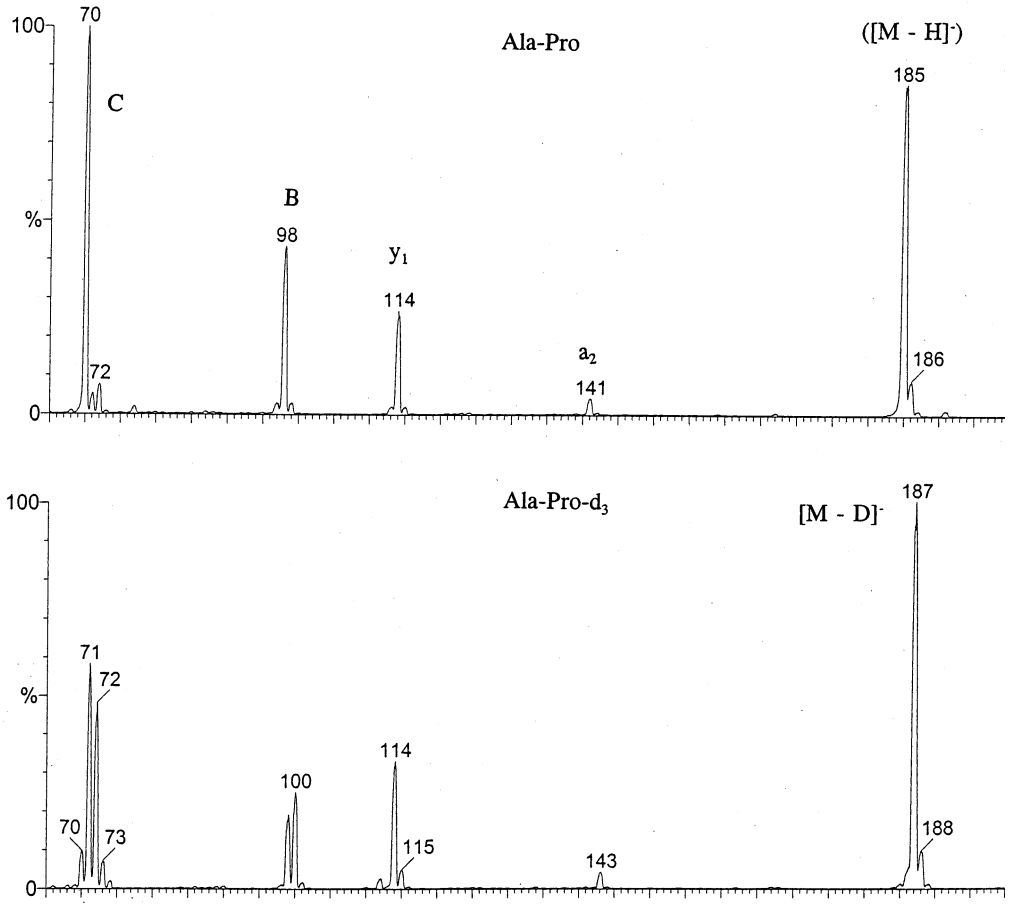

Figure 6. Comparison of CID mass spectra of $[M-H]^-$ of Ala-Pro and $[M-D]^-$ of Ala-Pro-d_3 (45-V cone voltage).

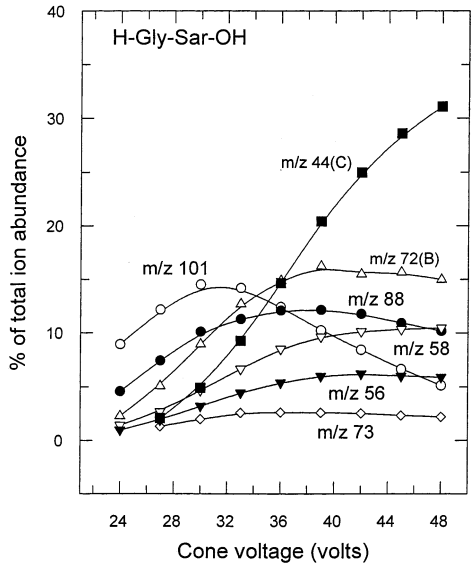

Figure 7. Breakdown graph for deprotonated Gly-Sar.

SCHEME 4

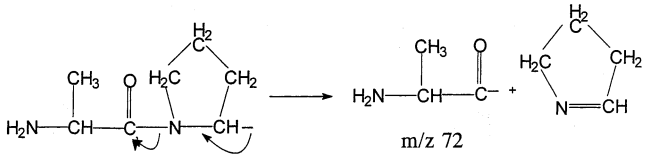

in the form of the potential energy diagram shown in Figure 10. Full structural parameters for each species can be found in the Supporting Information or obtained from the authors.

Experimentally it is not clear whether the a_2 ion derived from decarboxylation of deprotonated glycylglycine is formed in the trans (**1**) or the more stable cis (**2a**) configuration. There is a substantial barrier (14.1 kcal mol^{-1}) for conversion of the trans form **1** to the cis form **2a**. Structure **2a** reacts, as per Scheme 2, to abstract a proton from the N-terminal amino group through a transition state that is 8 kcal mol^{-1} higher in energy than **2**. This portion of the potential energy surface is similar to that reported by Styles and O'Hair.[29] The cis amino-deprotonated species **3** can then undergo fragmentation to form $[CH_3NHCO]^-$ + CH_2═NH, a reaction that is 23.8 kcal mol^{-1} endothermic. Alternatively, **3** might rearrange to the trans conformation **4** over a barrier of 11.7 kcal mol^{-1}. This trans species might fragment to the products $[CH_3NHCO]^-$ + CH_2═NH, or it might readily abstract a proton from the amidic nitrogen to form **5**, the most stable species on the $[C_3H_7N_2O]^-$ potential energy surface. It is very difficult to find the correct energy profile that contains a low-lying transition structure such as TS-4 that follows structure **4** and connects it with structure **5**. One of the reasons for this difficulty is that the surface is rather smooth and several low-lying minima might occur in the vicinity of the transition structure. If one locates one of the low-lying minima in the neighborhood as the reactant structure but it is not the lowest-energy conformer of the set, one might end up obtaining an apparently negative barrier. After a lengthy and careful search, we were able to optimize the true structure **4** connected to TS-4 and structure **5**, now making the barrier height associated with TS4 positive. However, when zero-point vibration energy is included, the relative stabilities are slightly reversed. It is therefore recommended that, in the construction

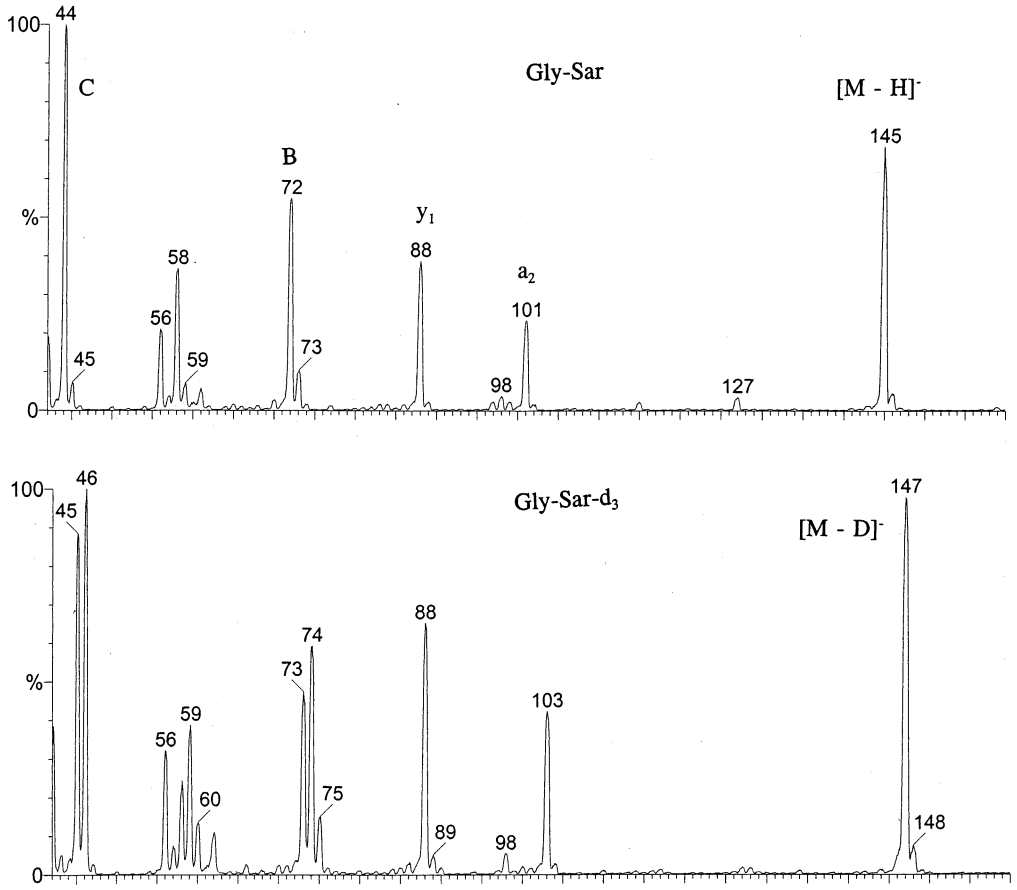

Figure 8. Comparison of CID mass spectra of $[M-H]^-$ of Gly-Sar and $[M-D]^-$ of Gly-Sar-d_3 (45-V cone voltage).

SCHEME 5

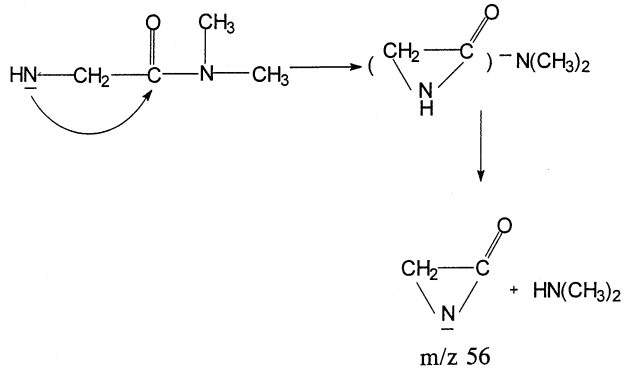

of energetic profiles or for any computations undertaken, care be taken to ensure that every conformer has been identified and evaluated. However, even then, when the barrier is in the vicinity of 1 kcal mol^{-1} or less, its value, with or without the zero-point correction, cannot be considered numerically reliable.

The CID experiments clearly are carried out under multiple-collision conditions, and it is most likely that more than one activating collision is required to achieve fragmentation. We suggest that the initial collision(s) lead to isomerization of **2a** to **5**, the global minimum, through the intermediacy of **3** and **4**. Because of the higher density of states for **5** at the isomerization energy and possibly because of deactivating collisions, the system effectively becomes trapped as structure **5**, and exchange of labile and C-bonded hydrogens does not occur. Structure **5** might interchange with structure **4**, but this does not lead to interchange of labile and C-bonded hydrogens. Upon an activating collision, **5** fragments to products by way of **4**. By

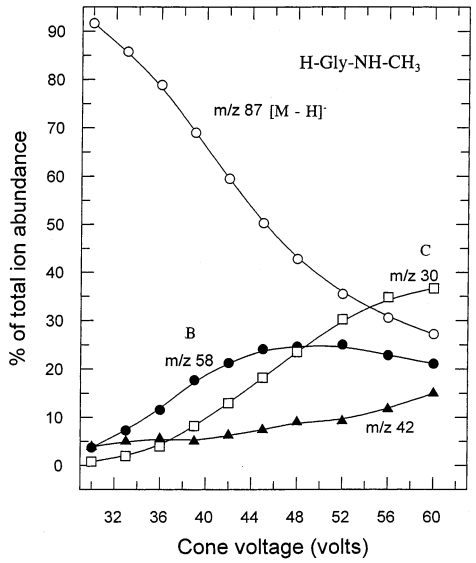

Figure 9. Breakdown graph for $[M-H]^-$ of H−Gly−$NHCH_3$.

contrast, when no amidic hydrogen is present, as in the a_2 ions derived from H−Ala−Pro−OH and H−Gly−Sar−OH, the structure analogous to **5** does not exist, and one observes an interchange of N-bonded and C-bonded hydrogens through the interconversion of structures analogous to **2a** and **3** because the barrier for this interconversion is lower than that for fragmentation.

We also have considered the possibility of direct conversion of **2a** to **5** by a 1,2-proton transfer. The calculations showed that this process had a high energy barrier, with the transition state (TS) being 93 kcal mol^{-1} (without the ZPE correction)

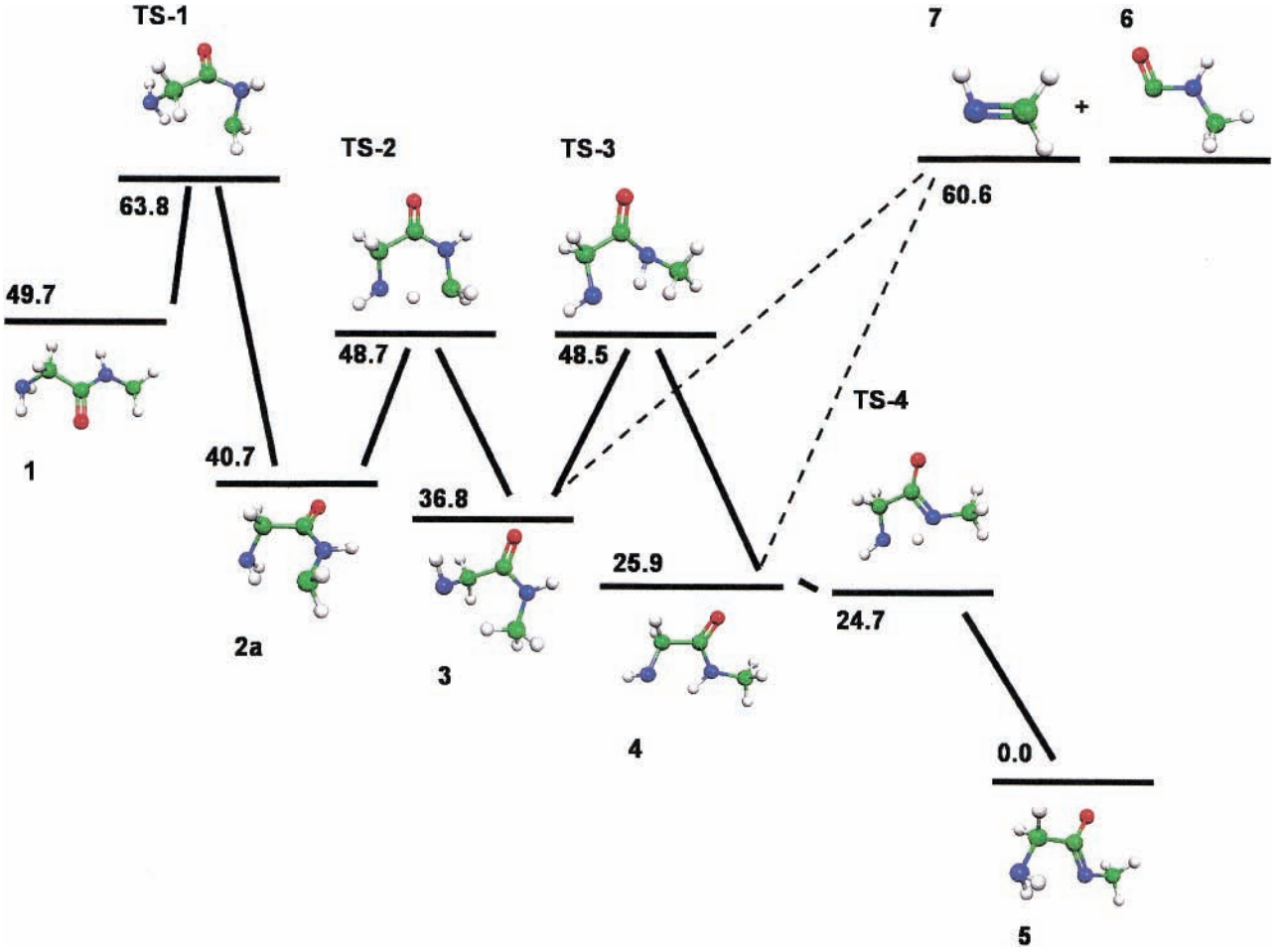

Figure 10. Potential energy surface for fragmentation of a_2 ion of Gly-Gly. **3** corresponds to A of Scheme 2, and **6** corresponds to B of Scheme 2. Relative energies in kcal mol^{-1}.

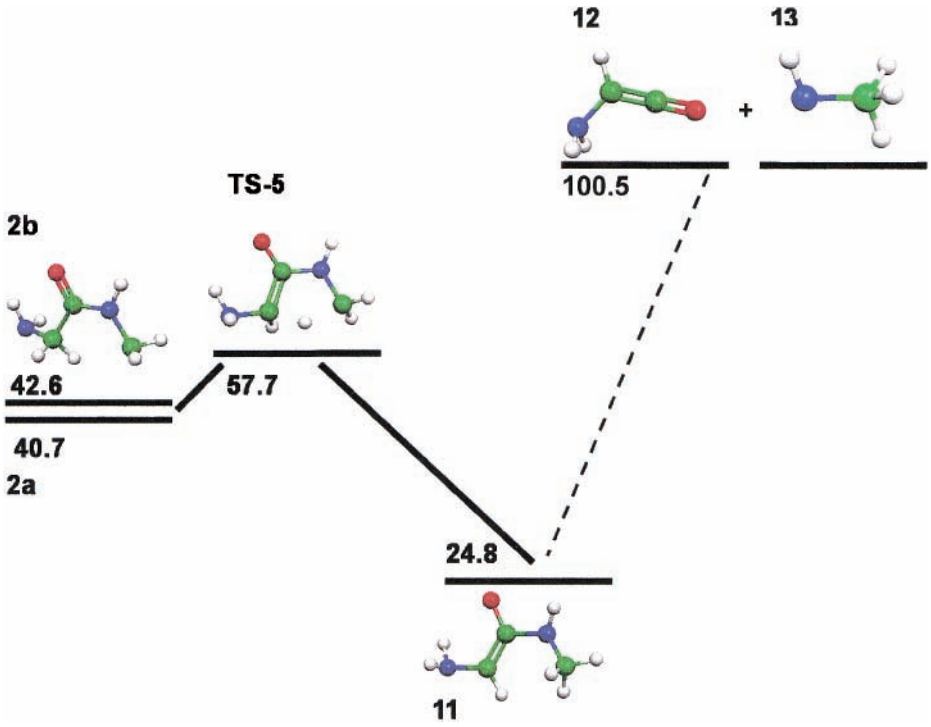

Figure 11. Potential energy surface for 1,4-proton transfer and fragmentation. Relative energies in kcal mol^{-1}.

above the energy of **2a**. Thus, this direct interconversion is not competitive with the multistep process illustrated in Figure 10.

A further experimental observation is that, when an amidic hydrogen is present, as in the a_2 ions derived from glycylglycine, glycylalanine, and alanylglycine, the elimination reaction 5 does

SCHEME 6

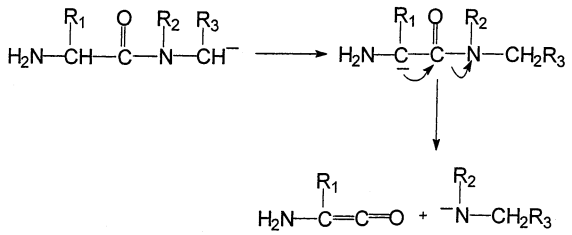

not occur to a significant extent

$$\underset{\textbf{2a/2b}}{H_2NCH_2C(=O)NHCH_2^-} \rightarrow \underset{\textbf{8}}{H_2NCH_2C(=O)^-} + \underset{\textbf{7}}{CH_2{=}NH}, \quad \Delta E = 27.6-29.5 \text{ kcal mol}^{-1} \quad (5)$$

On the other hand, when there is no amidic hydrogen, as in the a_2 ions derived from glycylsarcosine, the analogous reaction 6 does occur to a significant extent

$$\underset{\textbf{9}}{H_2NCH_2C(=O)N(CH_3)CH_2^-} \rightarrow \underset{\textbf{8}}{H_2NCH_2C(=O)^-} + \underset{\textbf{10}}{CH_3N{=}CH_2}, \quad \Delta E = 31.5 \text{ kcal mol}^{-1} \quad (6)$$

The most likely rationale for this difference is that, when an amidic hydrogen is present, the system becomes trapped in the low-energy states **4** and **5** and, on activation, exits only to **6** and **7**. Experimentally, when **5** is formed directly (Figure 9), this is what is observed. In effect, there is no significant population of **2a/b** to fragment by reaction 5. However, when no amidic hydrogen is present, exchange between the a_2 ion and the amine-deprotonated species occurs, with the result that there is a significant population of **9** that does fragment by reaction 6 on activation.

In contrast to the elimination of the N-terminal residue from a_n ($n \geq 3$) ions, where either a labile (N-bonded) or a nonlabile (C-bonded) proton can be transferred,[28] the present results indicate that specifically a labile (N-bonded) proton is transferred in the fragmentation of a_2 ions. Thus, the pathway outlined in Scheme 6, which leads directly to the deprotonated amine, is not involved. This pathway was explored by ab initio calculations for the a_2 ion derived from glycylglycine. The potential energy surface resulting from MP2/6-31+G(d) calculations is shown in Figure 11. The conformation of a_2 (**2b**) that leads to the possible 1,4-proton transfer is slightly higher in energy than the minimum-energy structure **2a**. The energy barrier leading from a_2 to the enolate ion **11** (17 kcal $\text{mol}^{-1-)}$ is considerably greater than that for proton abstraction from the amine group (8 kcal mol^{-1}, Figure 10). Consequently, it appears that the pathway outlined in Scheme 6 cannot compete with the pathway indicated by Figure 10. Further, the endothermicity for fragmentation of the enolate ion to the aminoketene and deprotonated amine is quite large. It might be that the barrier for proton abstraction from the enolate position in larger a_n ions is lower because a larger ring size is involved in the transition state.

The ab initio calculations that lead to Figures 10 and 11 can lead to estimates of the gas-phase acidities of the various positions in glycine *N*-methylamide. These estimates will be discussed in a forthcoming paper devoted to a more complete discussion of the theoretical calculations.

Acknowledgment. The authors are indebted to the Natural Sciences and Engineering Research Council (Canada) for financial support. Professor K. W. M. Siu (Centre for Research in Mass Spectrometry, York University) kindly provided access to the triple quadrupole mass spectrometer and Houssain El-Aribi expertly assisted with the MS^3 experiments. We also thank Azadi Mehdizadeh, Michelle A. Sahai, Jacqueline M. S. Law, David H. Setiadi, and Tania A. Pecora for helpful discussions, data extraction, and tabulation on the theoretical portion of this work. Special thanks is extended to Kenneth P. Chass of Velocet Communications Inc. for the contribution of the computational power and networking required for all calculations.

Supporting Information Available: Structural parameters and energies for species **1**−**13** and transition states TS-1−TS-5. This material is available free of charge via the Internet at http://pubs.acs.org.

References and Notes

(1) Hunt, D. F.; Yates, J. R., III; Shabanowitz, J.; Winston, S.; Hauer, C. R. *Proc. Natl. Acad. Sci. U.S.A.* **1986**, *83*, 6233.
(2) Biemann, K. *Methods Enzymol.* **1990**, *193*, 455.
(3) Biemann, K. In *Biological Mass Spectrometry: Present and Future*; Matsuo, T., Caprioli, R. M., Gross, M. L., Seyama, T., Eds.; Wiley: New York, 1993; p 275.
(4) Pappayanopoulos. I. *Mass Spectrom. Rev.* **1995**, *14*, 49.
(5) Roepstorff, P.; Fohlman, J. *Biomed. Mass Spectrom.* **1984**, *11*, 601.
(6) Biemann, K. *Biomed. Environ. Mass Spectrom.* **1988**, *16*, 99.
(7) O'Hair, R. A. J. *J. Mass Spectrom.* **2000**, *35*, 1377.
(8) Schlosser, A.; Lehmann, W. D. *J. Mass Spectrom.* **2000**, *35*, 1382.
(9) Polce, M. J.; Ren, D.; Wesdemiotis, C. *J. Mass Spectrom.* **2000**, *35*, 1391.
(10) Wysocki, V. H.; Tsaprailis, G.; Smith, L. L.; Breci, L. A. *J. Mass Spectrom.* **2000**, *35*, 1399.
(11) Bradley, C. V.; Howe, I.; Beynon, J. H. *J. Chem. Soc., Chem. Commun.* **1980**, 502.
(12) Bradley, C. V.; Howe, I.; Beynon. J. H. *Biomed. Mass Spectrom.* **1981**, *8*, 85.
(13) Kulik, W.; Heerma, W. *Biomed. Environ. Mass Spectrom.* **1988**, *17*, 173.
(14) Kulik, W.; Heerma, W. *Biomed. Environ. Mass Spectrom.* **1989**, *18*, 910.
(15) van Setten, D.; Kulik, W.; Heerma, W. *Biomed. Environ. Mass Spectrom.* **1990**, *19*, 475.
(16) Eckersley, M.; Bowie, J. H.; Hayes, R. N. *Org. Mass Spectrom.* **1989**, *24*, 597.
(17) Waugh, R. J.; Eckersley, M.; Bowie, J. H.; Hayes, R. N. *Int. J. Mass Spectrom. Ion Processes* **1990**, *98*, 135.
(18) Waugh, R. J.; Bowie, J. H.; Hayes, R. N. *Org. Mass Spectrom.* **1991**, *26*, 250.
(19) Waugh, R. J.; Bowie, J. H.; Hayes, R. N. *Int. J. Mass Spectrom. Ion Processes* **1991**, *107*, 333.
(20) Waugh, R. J.; Bowie, J. H.; Gross, M. L. *Aust. J. Chem.* **1993**, *46*, 693.
(21) Waugh, R. J.; Bowie, J. H.; Gross, M. L. *Rapid Commun. Mass Spectrom.* **1993**, *7*, 623.
(22) Reiter, A.; Teesch, L. M.; Zhao, H.; Adams, J. *Int. J. Mass Spectrom. Ion Processes* **1993**, *127*, 17.
(23) Marzluff, E. M.; Campbell, S.; Rodgers, M. T.; Beauchamp, J. L. *J. Am. Chem. Soc.* **1994**, *116*, 7787.
(24) Loo, J. A.; Ogorzalek Loo, R. R.; Light, K. L.; Edmonds, C. G.; Smith, R. D. *Anal. Chem.* **1992**, *64*, 81.
(25) Jai-nkuknan, J.; Cassady, C. J. *Anal. Chem.* **1998**, *70*, 5122.
(26) Jai-nkuknan, J.; Cassady, C. J. *Rapid Commun. Mass Spectrom.* **1996**, *10*, 1678.
(27) Ewing, N. P.; Cassady, C. J. *J. Am. Soc. Mass Spectrom.* **2001**, *12*, 105.
(28) Harrison, A. G. *J. Am. Soc. Mass Spectrom.* **2001**, *12*, 1.
(29) Styles, M. L.; O'Hair, R. A. J. *Rapid Commun. Mass Spectrom.* **1998**, *12*, 809.
(30) McLuckey, S. A,; Glish, G. L.; Cooks, R. G. *Int. J. Mass Spectrom. Ion Phys.* **1981**, *39*, 219.
(31) Fetterolf, D. D.; Yost, R. A. *Int. J. Mass Spectrom. Ion Phys.* **1982**, *44*, 37.
(32) McLuckey, S. A.; Cooks, R. G. In *Tandem Mass Spectrometry*; McLafferty, F. W., Ed.; Wiley: New York, 1983; p 203.
(33) Loo, J. A.; Udseth, R. D.; Smith, R. D. *Rapid Commun. Mass Spectrom.* **1988**, *2*, 207.
(34) Voyksner, T. D.; Pack, T. *Rapid Commun. Mass Spectrom.* **1991**, *5*, 263.

(35) Bruins, A. P. In *Electrospray Mass Spectrometry: Fundamentals, Instrumentation and Applications*; Cole, R. B., Ed.; Wiley: New York, 1997; Chapter 3.

(36) Donò, A.; Paradisi, C.; Scorrano, G. *Rapid Commun. Mass Spectrom.* **1997**, *11*, 1687.

(37) Collette, C.; DePauw, E. *Rapid Commun. Mass Spectrom.* **1998**, *12*, 165.

(38) Collette, C.; Drahos, L.; DePauw, E.; Vékey, K. *Rapid Commun. Mass Spectrom.***1998**, *12*, 1673.

(39) Harrison, A. G. *Rapid Commun. Mass Spectrom.* **1999**, *13*, 1663.

(40) van Dongen, W. D.; van Wijk, J. L. T.; Green, B. N.; Heerma, W.; Haverkamp, J. *Rapid Commun. Mass Spectrom.* **1999**, *13*, 1712.

(41) Harrison, A. G. *J. Mass Spectrom.* **1999**, *34*, 1253.

(42) Makowiecki, J.; Tolonen, A.; Uusitalo, J.; Jalonen, J. *Rapid Commun. Mass Spectrom.* **2001**, *15*, 1506.

(43) (a) Dewar, M. J. S.; Thiel, W. M. *J. Am. Chem. Soc.* **1977**, *99*, 4499. (b) Dewar, M. J. S.; Reynolds, C. H. *J. Comput. Chem.* **1986**, *2*, 140.

(44) (a) Møller, C.; Plesset, M. S. *Phys. Rev.* **1934**, *46*, 618. (b) Frisch, M. J.; Head-Gordon, M.; Pople, J. A. *Chem. Phys. Lett.* **1990**, *166*, 281.

(45) Csizmadia, I. G. In *New Theoretical Concepts for Understanding Organic Reactions*; Bertran, J., Ed.; Kluwer Academic Publishers: Dordrecht, The Netherlands, 1989; p 1.

(46) Ayala, P. Y.; Schlegel, H. B. *J. Chem. Phys.* **1997**, *107*, 375.

(47) Scott, A. P.; Radom, L. *J. Phys. Chem.* **1996**, *100*, 502.